IOPscience iopscience.iop.org

Home Search Collections Journals About Contact us My IOPscience

The analytic approach in the modelling of one-dimensional electron concentration distribution in some two-valley semiconductor electron devices

This article has been downloaded from IOPscience. Please scroll down to see the full text article.

1998 J. Phys. A: Math. Gen. 31 2997

(http://iopscience.iop.org/0305-4470/31/13/009)

View the table of contents for this issue, or go to the journal homepage for more

Download details:
IP Address: 171.66.16.121
The article was downloaded on 02/06/2010 at 06:30

Please note that terms and conditions apply.

J. Phys. A: Math. Gen. **31** (1998) 2997–3017. Printed in the UK PII: S0305-4470(98)87110-2

The analytic approach in the modelling of one-dimensional electron concentration distribution in some two-valley semiconductor electron devices

Bratislav D Iričanin† and Dejan M Gvozdić‡

University of Belgrade, Faculty of Electrical Engineering, Bulevar revolucije 73, PO Box 35–54, 11120 Belgrade, Yugoslavia

Received 26 August 1997, in final form 20 January 1998

Abstract. The conventional approach to the modelling of semiconductor devices operation is based on a numerical solution of transport equations. This paper exposes a complete analytical treatment of transport equations for a two-valley semiconductor. We consider the case when the geometry of the analysed structure permits us to assume that the transport in one of the dimensions of the structure is dominant, and when the electric field is homogeneous and stationary. The obtained solution for the case of generally set initial conditions is reduced to the quadratures. We used the example of a p-i-n diode to demonstrate the superiority of the analytical treatment as compared with the numerical one. The proposed approach offers the possibility to determine exactly and quickly the spatial-temporal distribution of the electron concentration within the structure. Considering the accuracy of the analytical procedure, compared with that of the numerical one, the obtained solution could also be used as a kind of standard for the analysis of particular approximate solutions of the considered type of partial differential equation systems.

1. Introduction

The modern methods used in semiconductor technology, such as molecular beam epitaxy (MBE) and metalorganic chemical vapour phase deposition (MOCVD), opened the possibility to increase the degree of integration in semiconductor integrated circuits and to fabricate submicron and nanostructure semiconductor devices. This caused a need for new mathematical and physical models of carrier transport which would be able to describe in detail the transport in such structures.

In modelling the operation of semiconductor devices with dimensions larger than one micrometer it is usual to apply the drift-diffusion model coupled with the Poisson's equation. This model is obtained by the integration of the classical Boltzmann equation, assuming that the carrier distribution can be described by a displaced Maxwell distribution [1]. However, this assumption is not fulfilled for devices that have submicron dimensions. In addition, the modelling of transport in semiconductor nanostructures is directly connected to quantum effects which require a fundamentally different approach from that in micron and submicron structures.

The electron transport in submicron semiconductor structures is mostly determined by nonstationary effects such as 'velocity overshoot' or 'ballistic transport' [1]. These

† E-mail address: iricanin@buef31.etf.bg.ac.yu
‡ E-mail address: gvozdic@kiklop.etf.bg.ac.yu

0305-4470/98/132997+21$19.50 © 1998 IOP Publishing Ltd

effects cannot be properly described by the classical drift-diffusion model. Therefore, the Monte Carlo simulation is employed [1] to obtain relatively satisfactory results. Nevertheless, due to the known limitations posed by the probabilistic approach and its high demands for computer processing time, it cannot remain the only method for analysis of transport processes. Another approach is based on the momentum method from which *the hydrodynamic model* of the transport equation is derived [1]. This model is also very complex to implement numerically, since it consists of a system of partial differential equations (PDEs) written in terms of carrier concentration, mean momentum and mean particle energy.

In two-valley semiconductors, such as GaAs, InGaAs and AlGaAs, electron transfer is predominantly influenced by intervalley transfer. The electron transport in this case is well described by the hydrodynamic model [2]. The hydrodynamic model for a two-valley semiconductor consists of a system of PDEs over carrier concentration, mean impulse and mean kinetic energy for each of the valleys. Instead of the equation over the mean particle (kinetic) energy it is possible to use an equivalent equation over mean temperature. Thus we describe the spatial-temporal distribution of electron temperature within a semiconductor device, as well as its influence on the distribution of the concentration itself, starting from the temperature-dependent relaxation times [2, 15, 16].

However, this model is very difficult to solve, which is the reason why its approximation—the so-called *phenomenological model*—is used instead [3–5]. The phenomenological model assumes that the stationary state for the kinetic degree of freedom is already established, but the process of electron distribution over the valleys is not yet completed. In this manner, the influence of electron temperature is implicitly taken into account over the transfer times $\tau_1(E)$ and $\tau_2(E)$ which are obtained using the Monte Carlo simulation.

This paper presents the analytical solution of the PDEs of the phenomenological model for the case when the structure of the semiconductor device permits us to approximate it by one-dimensional transport and when the electric field is stationary and homogeneous. The obtained solution is further applied in the special case of electron concentration profile determination in conduction band valleys within the absorption layer of a p-i-n photodiode. Finally, we present a comparison of the obtained exact solution with the conventional numerical solution [4, 5], with a detailed analysis of discrepancies.

2. The model

The phenomenological model describes the intervalley transport in the relaxation time or transfer time approximation, where these times are functions of the electric field [3–5]. The total electron concentration is determined by the electron concentrations in the central (Γ) valley n_1 and in the satellite (X, L) valleys n_2 of the conduction band. In our further consideration we assume that the electric field is stationary, homogeneous and strong enough so that electron diffusion can be neglected. In that case the electron velocity in each of the valleys is determined by the electric field intensity E and electron mobility for the particular valley μ_i:

$$\nu_i = \nu_i(E) = \mu_i(E)E \qquad (i = 1, 2) \tag{1}$$

where the index '1' corresponds to the central, and '2' to the satellite valleys of the conduction band. The electron velocity in the central valley is larger than in the satellite one ($\nu_1 > \nu_2$). The phenomenological model for electrons is defined by the following set

of PDEs with respect to the spatial-temporal concentration distribution:

$$\begin{aligned} \frac{\partial n_1}{\partial t} + v_1 \frac{\partial n_1}{\partial x} &= -\frac{n_1}{\tau_1} + \frac{n_2}{\tau_2} + G_1 - R_1 \\ \frac{\partial n_2}{\partial t} + v_2 \frac{\partial n_2}{\partial x} &= -\frac{n_2}{\tau_2} + \frac{n_1}{\tau_1} + G_2 - R_2. \end{aligned} \tag{2}$$

In equation (2) G_1 and G_2 denote generation, and R_1 and R_2 denote recombination terms for each of the valleys, the coefficients $\tau_1 = \tau_1(E)$ and $\tau_2 = \tau_2(E)$ are the electron transfer times from the central into the satellite valley (τ_1), and from the satellite into the central one (τ_2) [3–5].

In order to solve the PDE system (2) it is necessary to define initial and/or boundary conditions dependent on the structure of the semiconductor device and its mode of operation. In most of the semiconductor devices before the electric field is switched on charge carriers inhabit the central valley of the conduction band, while the satellite valleys are practically empty. Thus, the carrier distribution at the initial moment in the one-dimensional approximation can be set in the following manner:

$$\begin{aligned} n_1(x, 0) &= Cf(x)h(x) \\ n_2(x, 0) &= 0 \end{aligned} \tag{3}$$

where C is a constant, $f : [0, d] \rightarrow \mathbb{R}$ is an arbitrary function differentiable on the segment $[0, d]$ which, physically, represents the space of the semiconductor device under consideration, and $h(x)$ is the Heaviside function. Since the dimensions of the semiconductor devices are finite and most often the Dirichlet-type boundary conditions can be set at its boundaries, the $n_1(x, 0)$ is defined using $h(x)$. Such a situation is encountered in the case of a p-i-n photodiode with an absorption layer made of a two-valley semiconductor. Using this example we present the whole procedure of obtaining the analytical solution of the problem (2), (3), where d denotes the width of the absorption layer between the p-i-n photodiode contacts. Let us assume that at the initial moment electrons are generated by optical pulse excitation along the absorption layer only within the central valley, so that in (2) we have

$$\begin{aligned} G_1 &= Cf(x)h(x)\delta(t) \\ G_2 &= 0 \end{aligned} \tag{4}$$

where $\delta(t)$ is the Dirac delta function (with respect to time). Here, as well as in the rest of the text, we use that (customary) name although it would be more precise to apply the phrase, 'Dirac delta *distribution*'. We also assume that the concentration of photogenerated carriers is several orders of magnitude larger than equilibrium concentration. The relations (3) are obtained by integration of system (2) from $t = 0^-$ to $t = 0^+$, only accounting for relations (4). Accordingly, generation terms (4) lead to the initial conditions (3). Due to the very low recombination rate compared with the electron transport rate in two-valley semiconductors we assume that it can be neglected ($R_1 = R_2 = 0$). A similar treatment is applicable for other semiconductor devices where these basic assumptions are satisfied (MESFET, HEMT, etc).

3. Analytical treatment

The problem to be solved (2), (3) can be recognized as the Cauchy problem. For that purpose, the initial conditions are directly expanded in the following manner:

$$\begin{aligned} &n_1(x,0) = Cf(x)h(x) \\ &\frac{\partial n_1(x,0)}{\partial t} = -C\left(\left(\frac{f(x)}{\tau_1} + \nu_1 f'(x)\right)h(x) + \nu_1 f(x)\delta(x)\right) \\ &n_2(x,0) = 0 \\ &\frac{\partial n_2(x,0)}{\partial t} = \frac{C}{\tau_1} f(x)h(x). \end{aligned} \tag{5}$$

Let us try to transform the problem under consideration into a form more convenient for solving. We shall transform the PDE system into a second-order equation with respect to n_i, $(i = 1, 2)$. By removing the dependent variable n_2 from the system (2) we reduce it to the desirable second-order PDE over n_i:

$$\frac{\partial^2 n_1}{\partial t^2} + (\nu_1 + \nu_2)\frac{\partial^2 n_1}{\partial x \partial t} + \nu_1\nu_2\frac{\partial^2 n_1}{\partial x^2} + \left(\frac{\nu_1}{\tau_2} + \frac{\nu_2}{\tau_1}\right)\frac{\partial n_1}{\partial x} + \left(\frac{1}{\tau_1} + \frac{1}{\tau_2}\right)\frac{\partial n_1}{\partial t} = 0. \tag{6}$$

By introducing new independent variables α and β via the transformation

$$\alpha = x - \frac{\nu_1 + \nu_2}{2}t \qquad \beta = \frac{\nu_2 - \nu_1}{2}t \tag{7}$$

and by replacing n_1 by a new dependent variable w according to

$$n_1 = \exp(-(A+B)\alpha + (A-B)\beta)w(\alpha,\beta) \tag{8}$$

where

$$A = \frac{1}{\tau_1(\nu_1 - \nu_2)} \qquad B = -\frac{1}{\tau_2(\nu_1 - \nu_2)} \tag{9}$$

equation (6) assumes the following form:

$$\frac{\partial^2 w}{\partial \alpha^2} - \frac{\partial^2 w}{\partial \beta^2} + \frac{4}{\sqrt{\tau_1\tau_2}|\nu_1 - \nu_2|}w = 0. \tag{10}$$

The expanded initial conditions become

$$\begin{aligned} w_0(\alpha) &= w(\alpha,0) = C\exp((A+B)\alpha)\, f(\alpha)h(\alpha) = \psi_0^{(1)}(\alpha)h(\alpha) \\ w_1(\alpha) &= \frac{\partial w(\alpha,0)}{\partial \beta} = C\exp((A+B)\alpha) \\ &\quad \times \left(\left((A+B)f(\alpha) + \frac{2}{1-\nu_2/\nu_1}f'(\alpha)\right)h(\alpha) + \frac{2}{1-\nu_2/\nu_1}f(\alpha)\delta(\alpha)\right) \\ &= \psi_1^{(1)}(\alpha)h(\alpha) + \psi_2^{(1)}(\alpha)\delta(\alpha). \end{aligned} \tag{11}$$

The obtained problem (10), (11) is more convenient for solving than the initial problem (2)–(5). However, by introducing new independent variables

$$p = \alpha + \beta \qquad q = \alpha - \beta \tag{12}$$

equation (10) eventually becomes

$$\frac{\partial^2 w}{\partial p \partial q} + \frac{1}{\tau_1\tau_2(\nu_1 - \nu_2)^2}w = 0 \tag{13}$$

which is the most convenient one for solving. It is a *hyperbolic type* PDE with a self-adjoint inherent operator. The obtained equation is a special case of the so-called general *telegraphic equation* whose special cases are described in [6–8]. It is solved by using the Riemann method where we assume that the Riemann function V is

$$V(p,q;p_0,q_0) = r(z) \tag{14}$$

with

$$z = (p-p_0)(q-q_0) \tag{15}$$

$$V(q,q;q_0,q_0) = -1. \tag{16}$$

Under the assumption $z = \zeta^2$, the Bessel differential equation is obtained:

$$\frac{\partial^2 r}{\partial \zeta^2} + \frac{1}{\zeta}\frac{\partial r}{\partial \zeta} + r = 0 \tag{17}$$

with the corresponding particular solution $r(\zeta) = J_0(\zeta)$, where $J_n(x)$ denotes a Bessel function of the first kind of the nth order. By inversion of the applied transformations we find that the Riemann function is equal to

$$V = J_0\left(\frac{2}{\sqrt{\tau_1\tau_2}|\nu_1-\nu_2|}\sqrt{(x-\nu_1 t)(x-\nu_2 t)}\right). \tag{18}$$

For the solution of the PDE (10) with the initial conditions (11) we obtain

$$\begin{aligned} w(\alpha-\beta,\alpha+\beta) &= \tfrac{1}{2}(w_0(\alpha-\beta)+w_0(\alpha+\beta)) \\ &\quad +\frac{1}{2}\int_{\alpha-\beta}^{\alpha+\beta} J_0\left(\frac{2}{\sqrt{\tau_1\tau_2}|\nu_1-\nu_2|}\sqrt{(\alpha-\beta-\xi)(\alpha+\beta-\xi)}\right) w_1(\xi)\,\mathrm{d}\xi \\ &\quad -\frac{t}{2\tau_1\tau_2|\nu_1-\nu_2|}\int_{\alpha-\beta}^{\alpha+\beta} J_1\left(\frac{2}{\sqrt{\tau_1\tau_2}|\nu_1-\nu_2|}\sqrt{(\alpha-\beta-\xi)(\alpha+\beta-\xi)}\right) \\ &\quad \times w_0(\xi)\,\mathrm{d}\xi. \end{aligned} \tag{19}$$

Let us introduce a new variable θ:

$$\theta = 2\sqrt{\frac{-1}{\tau_1\tau_2(\nu_1-\nu_2)^2}(\alpha+\beta-\xi)(\alpha-\beta-\xi)}. \tag{20}$$

It stems from here that

$$\begin{aligned} \xi = \xi_j(\theta) &= \alpha + \frac{(-1)^j}{2}\sqrt{\tau_1\tau_2}|\nu_1-\nu_2|\sqrt{\left(\frac{t}{\sqrt{\tau_1\tau_2}}\right)^2 - \theta^2} \\ &= x - (\nu_1+\nu_2)\frac{t}{2} + \frac{(-1)j}{2}\sqrt{\tau_1\tau_2}|\nu_1-\nu_2|\sqrt{\left(\frac{t}{\sqrt{\tau_1\tau_2}}\right)^2 - \theta^2} \end{aligned} \tag{21}$$

where for $\alpha \geqslant \xi$ is $j = 1$, while $\alpha < \xi$ implies $j = 2$. From (20) it can be seen that $\theta \in [0, \frac{t}{\sqrt{\tau_1\tau_2}}]$, while for the variables ξ_j the following limitations are valid: $\xi_1 \in [x - \nu_1 t, x - \frac{\nu_1+\nu_2}{2}t]$ and $\xi_2 \in [x - \frac{\nu_1+\nu_2}{2}t, x - \nu_2 t]$. Now we transform the obtained solution (19) to enable its use for the starting problem. Also, we utilize the relation

$$I_n(z) = (-i)^n J_n(iz) \tag{22}$$

where $I_n(x)$ is the modified Bessel function of the first kind and nth order, valid for all complex values $z \in \mathbb{C}$. Each of the integrals in (19) can be separated into a sum of two

integrals with limits $\alpha - \beta$ and α (in the first one), and $\alpha, \alpha + \beta$ (in the second one), which brings us to the formula

$$w(x,t) = \tfrac{1}{2}(\psi_0^{(1)}(x - v_1 t)h(x - v_1 t) + \psi_0^{(1)}(x - v_2 t)h(x - v_2 t)) - \frac{\sqrt{\tau_1\tau_2}|v_1 - v_2|}{4}$$
$$\times \left(\int_0^{\frac{t}{\sqrt{\tau_1\tau_2}}} (\psi_1^{(1)}(\xi_1(\theta))h(\xi_1(\theta)) + \psi_1^{(1)}(\xi_2(\theta))h(\xi_2(\theta))) \frac{\theta I_0(\theta)\,\mathrm{d}\theta}{\sqrt{\left(\frac{t}{\sqrt{\tau_1\tau_2}}\right)^2 - \theta^2}} \right.$$
$$\left. + \int_0^{\frac{t}{\sqrt{\tau_1\tau_2}}} (\psi_2^{(1)}(\xi_1(\theta))\delta(\xi_1(\theta)) + \psi_2^{(1)}(\xi_2(\theta))\delta(\xi_2(\theta))) \frac{\theta I_0(\theta)\,\mathrm{d}\theta}{\sqrt{\left(\frac{t}{\sqrt{\tau_1\tau_2}}\right)^2 - \theta^2}} \right)$$
$$+ \frac{t}{2\sqrt{\tau_1\tau_2}} \int_0^{\frac{t}{\sqrt{\tau_1\tau_2}}} (\psi_0^{(1)}(\xi_1(\theta))h(\xi_1(\theta)) + \psi_0^{(1)}(\xi_2(\theta))h(\xi_2(\theta)))$$
$$\times \frac{I_1(\theta)\,\mathrm{d}\theta}{\sqrt{\left(\frac{t}{\sqrt{\tau_1\tau_2}}\right)^2 - \theta^2}}. \tag{23}$$

Let us mention that the bottom limit of these integrals corresponds to $\alpha - \beta$ and $\alpha + \beta$, and the upper limit to the variable α in formula (19).

Now we analyse the Heaviside factors in the integrand functions of the solution (23). Depending on their non-zero values, the solution (spatial-temporal dependence) can be separated into four parts (not forgetting that x and t cannot be negative). In the first region $x > v_1 t$ is valid; here the values of the Heaviside functions are $h(\xi_1(\theta)) = h(\xi_2(\theta)) = 1$. The second region is described by the inequalities $\frac{v_1+v_2}{2}t < x \leqslant v_1 t$ and in it is

$$h(\xi_1(\theta)) = \begin{cases} 0 & \theta < \theta_c \\ 1 & \theta > \theta_c \end{cases}$$

while $h(\xi_2(\theta)) = 1$ (in the whole region). The third region is characterized by the relation $v_2 t < x \leqslant \frac{v_1+v_2}{2}t$, and there is

$$h(\xi_2(\theta)) = \begin{cases} 0 & \theta > \theta_c \\ 1 & \theta < \theta_c \end{cases}$$

and $h(\xi_1(\theta)) = 0$ (in the whole region). In the remaining, fourth region is $x \leqslant v_2 t$ and the values of the Heaviside functions here are $h(\xi_1(\theta)) = h(\xi_2(\theta)) = 0$. In our previous consideration we have introduced a cut-off value θ_c of the variable θ, equal to

$$\theta_c = \frac{2}{\sqrt{\tau_1\tau_2}|v_1 - v_2|}\sqrt{(v_1 t - x)(x - v_2 t)}. \tag{24}$$

Now in (23) only those addends remain for which the factor $h(\xi_i(\theta)) = 1$, $(i = 1, 2)$. This suggests that the solution itself can be separated into four different expressions valid in particular regions which are shown in figure 1.

Using the property of the Dirac δ-function

$$\int_a^b \delta(x)\,\mathrm{d}x = \begin{cases} 0 & 0 \notin [a,b] \\ 1 & 0 \in [a,b] \end{cases} \tag{25}$$

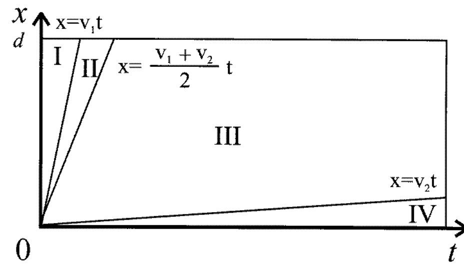

Figure 1. Regions (I–IV) in the spatial-temporal dependence.

which stems directly from its definition we conclude that the result of the integration of the part of the integrand which includes $\delta(\xi_1(\theta))$ or $\delta(\xi_2(\theta))$ only depends on whether or not the functions $\xi_1(\theta)$ and $\xi_2(\theta)$ reach zero in the segment $\theta \in \left[0, \frac{t}{\sqrt{\tau_1\tau_2}}\right]$ for the considered values of the variable x. If these functions are not equal to zero within this segment, the integral of this part of the integrand will be equal to zero. This is just what happens in regions I and IV. In regions II and III the functions $\xi_1(\theta)$ and $\xi_2(\theta)$ change their signs, as established by the previous analysis of Heaviside functions, so that in these regions the integrals are non-zero.

Finally, by convenient rearrangement of the addends in the integrated expression, the obtained solution is reduced to the following formulae:

- for $x > \nu_1 t$

$$w(x,t) = \frac{1}{2}(\psi_0^{(1)}(x-\nu_1 t) + \psi_0^{(1)}(x-\nu_2 t)) + F_1\left(0, \frac{t}{\sqrt{\tau_1\tau_2}}\right) + F_2\left(0, \frac{t}{\sqrt{\tau_1\tau_2}}\right) \qquad (26a)$$

- for $\nu_1 t \geqslant x > \frac{\nu_1+\nu_2}{2}t$

$$w(x,t) = \frac{1}{2}\psi_0^{(1)}(x-\nu_2 t) + F_1\left(\theta_c, \frac{t}{\sqrt{\tau_1\tau_2}}\right) - D(\theta_c, t) + F_2\left(0, \frac{t}{\sqrt{\tau_1\tau_2}}\right) \qquad (26b)$$

- for $\frac{\nu_1+\nu_2}{2}t \geqslant x > \nu_2 t$

$$w(x,t) = \tfrac{1}{2}\psi_0^{(1)}(x-\nu_2 t) + F_2(0,\theta_c) - D(\theta_c, t) \qquad (26c)$$

- for $\nu_2 t \geqslant x \geqslant 0$

$$w(x,t) = 0 \qquad (26d)$$

which will be additionally elucidated. We define the functions $F_i(a,b)$ as integrals given by the following expressions:

$$F_i(a,b) = \int_a^b \frac{p_{fi}(\theta)\,\mathrm{d}\theta}{\sqrt{\left(\frac{t}{\sqrt{\tau_1\tau_2}}\right)^2 - \theta^2}} \qquad (27)$$

where

$$p_{fi}(\theta) = -\frac{\sqrt{\tau_1\tau_2}}{4}|\nu_1-\nu_2|\theta I_0(\theta)\psi_1^{(1)}(\xi_i(\theta)) + \frac{1}{2}\frac{t}{\sqrt{\tau_1\tau_2}} I_1(\theta)\psi_0^{(1)}(\xi_i(\theta)). \qquad (28)$$

Recall that the functions $\psi_0^{(1)}$ and $\psi_1^{(1)}$ are defined in the transformed expanded initial conditions (11). The functions $F_i(a,b)$ have been introduced to make the expression of the solution (26*a*–*d*) less comprehensive, but they are also algorithmically convenient from the aspect of software implementation.

Consequently, from the nature of initial conditions, namely the part of the integrand comprising the Dirac δ-functions $\delta(\xi_1(\theta))$ and $\delta(\xi_2(\theta))$, the addend $D(\theta_c, t)$ in (26*b*, *c*) is

$$D(\theta_c, t) = \frac{C\nu_1\sqrt{\tau_1\tau_2}}{2}\frac{\theta_c I_0(\theta_c) f(0)}{\sqrt{\left(\frac{t}{\sqrt{\tau_1\tau_2}}\right)^2 - \theta_c^2}}. \tag{29}$$

In expression (27) we calculate the principal value (v.p.) of the integral (in Cauchy sense) in the case of a singularity in the upper boundary.

Finally,

$$n_1(x, t) = \mathrm{e}^{k_x x + k_t t} w(x, t) \tag{30}$$

where the exponential coefficients are

$$\begin{aligned} k_x &= \frac{\tau_1 - \tau_2}{\tau_1\tau_2(\nu_1 - \nu_2)} \\ k_t &= \frac{\nu_2\tau_2 - \nu_1\tau_1}{\tau_1\tau_2(\nu_1 - \nu_2)} \end{aligned} \tag{31}$$

which originated from expressions (7)–(9).

The solution for the function n_2 can be obtained by an analogous procedure, bearing in mind that the starting system is reduced to the same equation (10) or (13). The difference is that the expanded initial conditions are in this case

$$\begin{aligned} w_0(\alpha) &= w(\alpha, 0) = 0 \\ w_1(\alpha) &= \frac{\partial w(\alpha, 0)}{\partial\beta} = -2CA\exp((A+B)\alpha) f(\alpha)h(\alpha) = \psi_1^{(2)}(\alpha)h(\alpha). \end{aligned} \tag{32}$$

The following formulae are obtained:

- for $x > \nu_1 t$

$$n_2(x, t) = \mathrm{e}^{k_x x + k_t t}\left(H_1\left(0, \frac{t}{\sqrt{\tau_1\tau_2}}\right) + H_2\left(0, \frac{t}{\sqrt{\tau_1\tau_2}}\right)\right) \tag{33a}$$

- for $\nu_1 t \geqslant x > \frac{\nu_1+\nu_2}{2}t$

$$n_2(x, t) = \mathrm{e}^{k_x x + k_t t}\left(H_1\left(\theta_c, \frac{t}{\sqrt{\tau_1\tau_2}}\right) + H_2\left(0, \frac{t}{\sqrt{\tau_1\tau_2}}\right)\right) \tag{33b}$$

- for $\frac{\nu_1+\nu_2}{2}t \geqslant x > \nu_2 t$

$$n_2(x, t) = \mathrm{e}^{k_x x + k_t t} H_2(0, \theta_c) \tag{33c}$$

- for $\nu_2 t \geqslant x \geqslant 0$

$$n_2(x, t) = 0. \tag{33d}$$

The integrals $H_i(a, b)$ are defined in the following manner:

$$H_i(a, b) = -\frac{\sqrt{\tau_1\tau_2}|\nu_1 - \nu_2|}{4}\int_a^b \frac{p_{hi}(\theta)\,\mathrm{d}\theta}{\sqrt{\left(\frac{t}{\sqrt{\tau_1\tau_2}}\right)^2 - \theta^2}} \tag{34}$$

where the well-behaved part of the integrand function is equal to

$$p_{hi}(\theta) = \theta I_0(\theta)\psi_1^{(2)}(\xi_i(\theta)). \tag{35}$$

In this manner we practically conclude the analytic solution procedure, where the obtained solutions for $n_1(x, t)$ and $n_2(x, t)$ are continuous functions.

However, note that some of the integrals in (27) and (34) are improper. Their form is

$$P(a,b)=\int_a^b \frac{p(\theta)\,\mathrm{d}\theta}{\sqrt{c^2-\theta^2}} \qquad (b\leqslant c) \tag{36}$$

and it can be seen that for $c=b$ they are singular in the upper boundary. This singularity has the form of an inverse square root. Therefore, the singularity is removable. By substituting

$$\theta = b-\vartheta^2 \tag{37}$$

in the integral (36), we obtain

$$P(a,b)=-2\int_{\sqrt{b-a}}^{0}\frac{p(b-\vartheta^2)}{\sqrt{2b-\vartheta^2}}\mathrm{sgn}\vartheta\,\mathrm{d}\vartheta = 2\int_0^{\sqrt{b-a}}\frac{p(b-\vartheta^2)}{\sqrt{2b-\vartheta^2}}\,\mathrm{d}\vartheta \tag{38}$$

because the new variable ϑ cannot be negative. Now we can calculate the obtained integrals by some of the standard methods of numerical integration, taking care about the nature of the integrand function.

Let us note that in the analytical solution (for which it is said to be solved in quadratures) there is nevertheless a part which should be calculated approximately, and this part is the value of the integral. However, bearing in mind the complexity (the order) of the required approximate methods and knowing which integrals and starting equations we are dealing with, we conclude that the proposed methods offer an essential improvement in comparison with the methods utilized until now in the analysis of the phenomena under consideration by approximate solution of some special cases of the Cauchy problem (2)–(5).

4. An example of the modelling of a semiconductor device

The proposed exact treatment of the model described by the PDE system (2) and by the initial conditions of general type (3) or (5) gives results potentially applicable in the modelling of electron transport in semiconductor electron devices. We demonstrate the efficiency of the analytical approach in the example of a p-i-n photodiode with the absorption layer made of a two-valley semiconductor (GaAs, InGaAs, AlGaAs). This efficiency is reflected not only in the quantitative (numerical) superiority, but also in the possibility to create a qualitatively clearer and more detailed picture of carrier transport mechanisms in such semiconductors. The advantage in rapidity of reaching the solution (i.e. the number of performed computer operations) is evident, but we did not measure it explicitly, since the numerical processes involved are incomparable [9]. It follows from the fact that the numerical method requires all the previous calculations in the discretization mesh, as opposed to the analytical one. The quality of the analytical solution became fully visible in the comparative analysis with the approximate solution obtained by purely numerical treatment of the starting equations using the finite difference method.

Let us consider the situation corresponding to the case of homogeneous distribution of photogenerated charge along the photodiode absorption layer at the moment $t=0$. This situation occurs when the reciprocal value of the absorption coefficient α is much smaller than the absorption layer width ($\alpha^{-1}\ll d$). In this case the function describing the initial conditions is constant, i.e. $f(x)\equiv 1$.

4.1. Application of the analytical treatment

In the following we present the analytical solution obtained in section 3, corresponding to the particular case $f(x)\equiv 1$. Under this condition the analytical solution can be rewritten in a much more compact form which is simpler for effective calculations.

First, the expanded initial conditions (5) now become

$$\begin{aligned} &n_1(x,0) = Ch(x)\\ &\frac{\partial n_1(x,0)}{\partial t} = -\frac{C}{\tau_1}h(x) - C\nu_1\delta(x)\\ &n_2(x,0) = 0\\ &\frac{\partial n_2(x,0)}{\partial t} = \frac{C}{\tau_1}h(x) \end{aligned} \tag{39}$$

while the equalities (11) and (32) are reduced to the equalities (40) and (41):

$$\begin{aligned} w_0(\alpha) &= w(\alpha,0) = C\exp\left((A+B)\alpha\right)h(\alpha) = \psi_0^{(1)}(\alpha)h(\alpha)\\ w_1(\alpha) &= \frac{\partial w(\alpha,0)}{\partial\beta} = C\exp\left((A+B)\alpha\right)\left((A+B)h(\alpha) + \frac{2}{1-\nu_2/\nu_1}\delta(\alpha)\right)\\ &= \psi_1^{(1)}(\alpha)h(\alpha) + \psi_2^{(1)}(\alpha)\delta(\alpha) \end{aligned} \tag{40}$$

$$\begin{aligned} w_0(\alpha) &= w(\alpha,0) = 0\\ w_1(\alpha) &= \frac{\partial w(\alpha,0)}{\partial\beta} = -2CA\exp\left((A+B)\alpha\right)h(\alpha) = \psi_1^{(2)}(\alpha)h(\alpha) \end{aligned} \tag{41}$$

respectively. We present the expressions (26*a*–*d*) and (33*a*–*d*) for concentrations n_1 and n_2 in a form which is compact and thus more convenient for qualitative consideration. After a number of algebraic transformations, the expressions for the concentrations n_1 and n_2 are obtained:

- for $x > \nu_1 t$

$$n_1(x,t) = C\left(\frac{1}{1+\tau_2/\tau_1} + \frac{1}{1+\tau_1/\tau_2}e^{-t\frac{\tau_1+\tau_2}{\tau_1\tau_2}}\right) \tag{42a}$$

$$n_2(x,t) = \frac{C}{1+\tau_1/\tau_2}(1 - e^{-t\frac{\tau_1+\tau_2}{\tau_1\tau_2}}) \tag{42b}$$

- for $\nu_1 t \geqslant x > \frac{\nu_1+\nu_2}{2}t$

$$n_1(x,t) = C\left(\frac{1}{1+\tau_2/\tau_1} + \frac{1}{1+\tau_1/\tau_2}e^{-t\frac{\tau_1+\tau_2}{\tau_1\tau_2}} - \frac{1}{2}e^{-\frac{t}{\tau_1}}\right) - e^{k_x x + k_t t}F_1(0,\theta_c) \tag{43a}$$

$$n_2(x,t) = \frac{C}{1+\tau_1/\tau_2}\left(1 - e^{-t\frac{\tau_1+\tau_2}{\tau_1\tau_2}}\right) - e^{k_x x + k_t t}H_1(0,\theta_c) \tag{43b}$$

- for $\frac{\nu_1+\nu_2}{2}t \geqslant x > \nu_2 t$

$$n_1(x,t) = \frac{C}{2}e^{-\frac{t}{\tau_2}} + e^{k_x x + k_t t}F_2(0,\theta)c) \tag{44a}$$

$$n_2(x,t) = e^{k_x x + k_t t}H_2(0,\theta_c) \tag{44b}$$

- for $\nu_2 t \geqslant x \geqslant 0$

$$n_1(x,t) = 0 \tag{45a}$$

$$n_2(x,t) = 0. \tag{45b}$$

In establishing the expressions (43*a*–*b*) and (44*a*–*b*) we took into account that the addend (29), stemming from the nature of the initial conditions, has a small influence on the obtained concentration values and can be neglected. It is the consequence of the

numerical values of the constants and, generally speaking, it could not be fulfilled. Besides the known equalities, we used in the previous expressions the following identities (cf [10]):

$$\int_0^{\frac{t}{\sqrt{\tau_1\tau_2}}} \cosh\left(\frac{\tau_2-\tau_1}{2\sqrt{\tau_1\tau_2}}\sqrt{\left(\frac{t}{\sqrt{\tau_1\tau_2}}\right)^2-\theta^2}\right)\frac{I_1(\theta)\,\mathrm{d}\theta}{\sqrt{\left(\frac{t}{\sqrt{\tau_1\tau_2}}\right)^2-\theta^2}} = \frac{\sqrt{\tau_1\tau_2}}{t}\left(\cosh\frac{t}{2}\frac{\tau_1+\tau_2}{\tau_1\tau_2}-\cosh\frac{t}{2}\frac{\tau_1-\tau_2}{\tau_1\tau_2}\right) \tag{46}$$

$$\int_0^{\frac{t}{\sqrt{\tau_1\tau_2}}} \cosh\left(\frac{\tau_2-\tau_1}{2\sqrt{\tau_1\tau_2}}\sqrt{\left(\frac{t}{\sqrt{\tau_1\tau_2}}\right)^2-\theta^2}\right)\frac{\theta I_0(\theta)\,\mathrm{d}\theta}{\sqrt{\left(\frac{t}{\sqrt{\tau_1\tau_2}}\right)^2-\theta^2}} = 2\frac{\sqrt{\tau_1\tau_2}}{\tau_1+\tau_2}\sinh\frac{t}{2}\frac{\tau_1+\tau_2}{\tau_1\tau_2}. \tag{47}$$

Owing to (46) and (47), in this—special—case we have removed all the possibly existing singularities in the integrals (27) and (34).

Regarding the remaining numerical integration (on the interval $(0, \theta_c)$) we used Romberg's method [11], and special care has been granted to the calculation of the values of modified Bessel functions (due to [12]).

Based on the comparative analysis of the exact (analytical) and approximate (numerical) approach to this task we substantiate the generality and advantages of the first one.

4.2. Numerical treatment

The PDE system (2), or the equivalent PDE (10) (a detailed analysis of such PDEs is given in [13]) is *hyperbolic*. There are various methods which can be applied in numerical calculation of the approximate solution of both the starting and the transformed problem (10), (11). In our research we decided to use the method of finite differences directly applied to the initial problem (2), (5). Since these equations describe the carrier flow, the choice of the scheme and the discretization steps should be performed to accurately describe the transport process in each step. One of the schemes to be found in literature is the so-called *upwind* scheme [14]. It uses the form of back finite differences and it has shown good results in the treatment of similar phenomena in the modelling of two-valley semiconductor devices [4,5]. The discretization steps over time Δt and position Δx must fulfil the stability criterion which is given here by

$$\Delta x \geqslant \Delta t \max_i\{v_i\}. \tag{48}$$

In the proposed finite difference form the problem (2)–(5) becomes the following system of difference equations:

$$\begin{aligned}\frac{(n_1^*)_j^{k+1}-(n_1^*)_j^k}{\Delta t}+\frac{v_1(n_1^*)_j^k-v_1(n_1^*)_{j-1}^k}{\Delta x} &= -\frac{(n_1^*)_j^k}{\tau_1}+\frac{(n_2^*)_j^k}{\tau_2}\\ \frac{(n_2^*)_j^{k+1}-(n_2^*)_j^k}{\Delta t}+\frac{v_2(n_2^*)_j^k-v_2(n_2^*)_{j-1}^k}{\Delta x} &= -\frac{(n_2^*)_j^k}{\tau_2}+\frac{(n_1^*)_j^k}{\tau_1}\end{aligned} \tag{49}$$

with the initial conditions

$$\begin{aligned}(n_1^*)_j^0 &= C\\ (n_2^*)_j^0 &= 0\end{aligned} \tag{50}$$

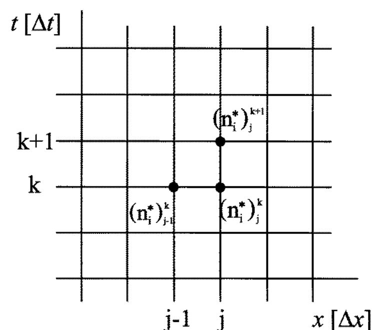

Figure 2. Mesh-point for the upwind scheme for numerical calculation of the PDE system (2) using (49) in terms of $n_i^*(x,t)$, $(i=1,2)$.

(for all j), where Δt and Δx are conveniently chosen discretization steps, and $n_i^* = n_i^*(x,t)$, $(i = 1,2)$, numerically obtained solutions for concentrations. Figure 2 shows schematically the mesh-point relevant in each step. In our calculations we adopted the values $x = 0$ (12.5×10^{-3}) 5 μm and $t = 0$ (10^{-3}) 60 ps, $C = 1$. Thus, we obtained the values of the normalized concentration in the conduction band valleys.

4.3. The comparative analysis of analytical and numerical solutions with physical consequences

From the obtained relatively simple equations (42*a*)–(45*a*) and (42*b*)–(45*b*) it can be observed that there is a general exponential time dependence of concentration. Explicit formulae (42*a*)–(45*a*) and (42*b*)–(45*b*) point to a certain effect which cannot be observed from the numerically obtained solutions. In those equations there is a new time constant describing the concentrations in the valleys of the conduction band. It is equal to half of the harmonic mean of the time constants τ_1 and τ_2. This explicitly shows the manner of transfer times τ_1 and τ_2 electron concentration distribution in each of the valleys. In regions I and IV the obtained solution does not depend on the variable x. This is a consequence of specific initial conditions determined by a constant function f. In contrast, in the remaining regions (II and III) that dependence exists. Besides that, in expressions (43), (44) there is an implicit dependence of carrier velocity ν_1 and ν_2, which can be seen in formulae (31), (27), (34) and (24). Only the analytical approach shows that within the region where $x > \nu_1 t$ the following asymptotic relations are valid:

$$n_1 \to \frac{C}{1+\tau_2/\tau_1} \qquad n_2 \to \frac{C}{1+\tau_1/\tau_2} \tag{51}$$

$(t \to \infty)$, while generally (in the other regions) the following is valid:

$$n_1 \to 0 \qquad n_2 \to 0. \tag{52}$$

However, the relations (51) could be obtained from equation (2), but the restriction for the range of the validity of (51) could not be perceived only considering them. Otherwise, relations (51) and (52) describe the saturation process.

We performed a comparative analysis of our analytical and standard numerical solution for three representative values of the parameter (electric field intensity E): for weak (5 kV cm^{-1}), intermediate (10 kV cm^{-1}) and strong (30 kV cm^{-1}) fields activity, when electron 'heating' in the semiconductor is intensive.

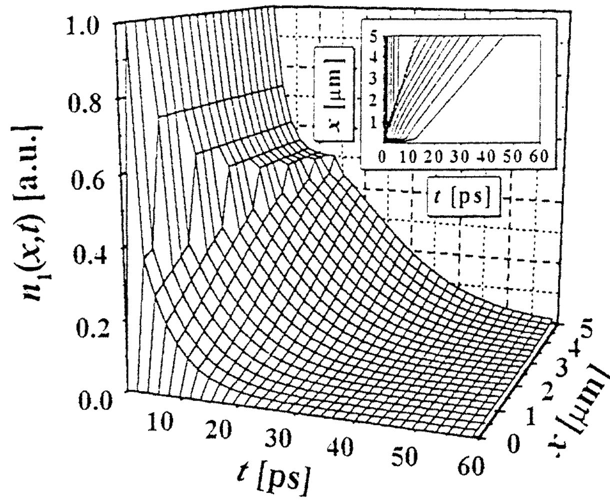

Figure 3. Spatial-temporal distribution of normalized concentration $n_1(x, t)$ in the central (Γ) valley for electric field $E = 5$ kV cm^{-1}.

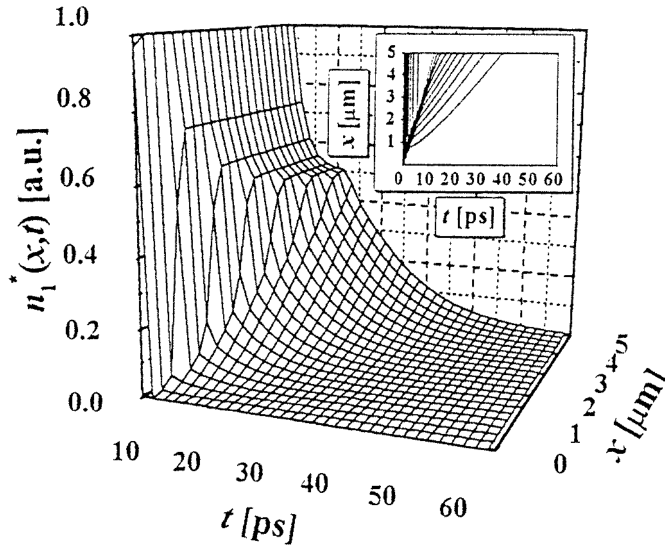

Figure 4. Spatial-temporal distribution of normalized concentration $n_1^*(x, t)$ in the central (Γ) valley for electric field $E = 5$ kV cm^{-1}.

Figures 3, 6, 9 and 12 are the graphical illustrations of the concentrations n_1 and n_2 (obtained according to section 4.1) for characteristic parameter values in a two-valley semiconductor according to [4, 5] ($\tau_2 = 5$ ps), as well as for maximal values of x ($\leqslant d = 5$ μ m) and t ($\leqslant 60$ ps) relevant for the optoelectronic devices designed utilizing this principle. Figures 4, 7, 10 and 13 show numerically obtained concentrations n_1^* and n_2^* (section 4.2) and figures 5, 8, 11 and 14 depict the values of spatial-temporal distribution of absolute errors $\epsilon_1 = n_1 - n_1^*$ and $\epsilon_2 = n_2 - n_2^*$.

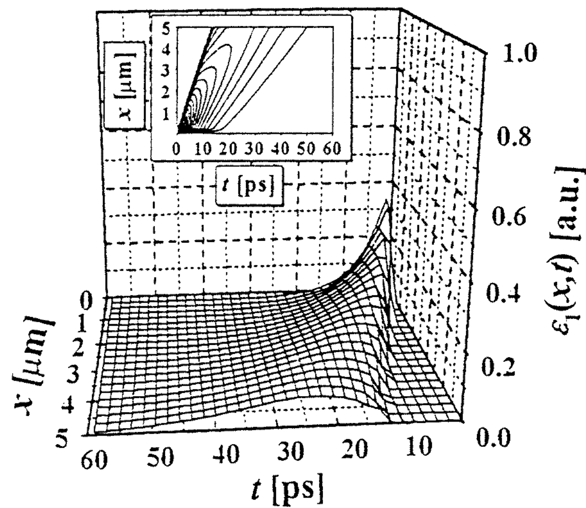

Figure 5. Spatial-temporal distribution of the difference $\epsilon_1(x,t)$ of the obtained concentrations in the central (Γ) valley for electric field $E = 5$ kV cm^{-1}.

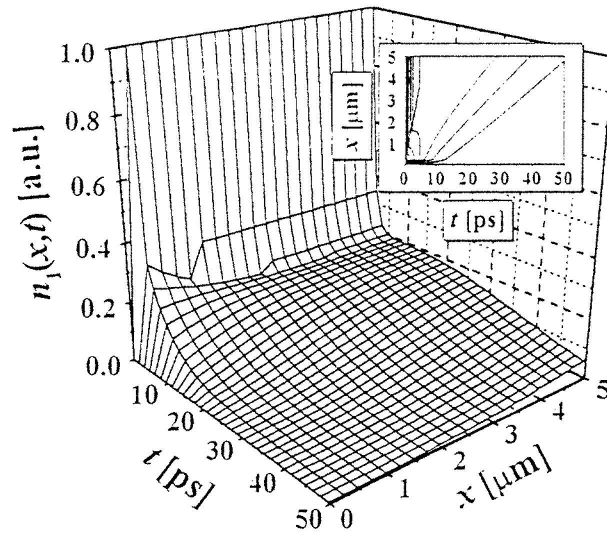

Figure 6. Spatial-temporal distribution of normalized concentration $n_1(x,t)$ in the central (Γ) valley for electric field $E = 10$ kV cm^{-1}.

When we consider weak electric fields, the intervalley transfer between the conduction band valleys exists, but is significantly less intensive than in the case of strong fields. Those carriers not scattered by the electric field and remaining in the central valley during transport move much faster than the carriers in the satellite valleys. It is a consequence of the lower effective mass, i.e. higher mobility, which is two orders of magnitude higher in the central valley than in the satellite ones. Such carriers leave the semiconductor very quickly. Their transport determines the region in which the relation $x > v_1 t$ is valid (region I; see figure 1) in the analytical solution. The carriers scattered from the central valley into the

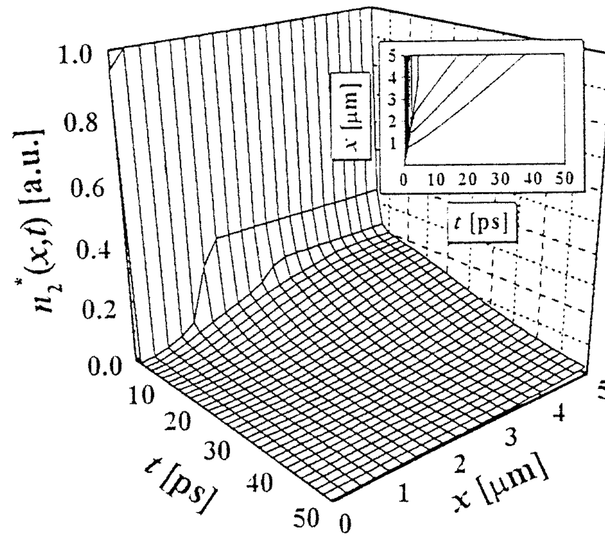

Figure 7. Spatial-temporal distribution of normalized concentration $n_1^*(x, t)$ in the central (Γ) valley for electric field $E = 10$ kV cm^{-1}.

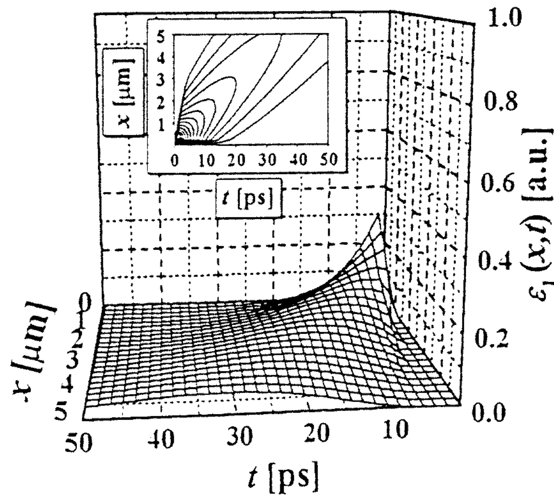

Figure 8. Spatial-temporal distribution of the difference $\epsilon_1(x, t)$ of the obtained concentrations in the central (Γ) valley for electric field $E = 10$ kV cm^{-1}.

satellite valleys return into the central valley. The flow of these carriers is described by the expressions corresponding to the region where $\nu_2 t < x < \nu_1 t$ (regions II and III). This means that the carrier transport proceeds through the central valley, while the intervalley transfer can be represented as a kind of a 'braking' mechanism.

In the strong electric field the transport mechanism is similar, but the intervalley transfer becomes so strong that electrons are transferred into the satellite valley in a very short time, while the central valley remains practically empty. The carrier transport continues to proceed via the central valley, and due to the strong electric field the electrons returned from the satellite valley into the central valley quickly go back into the satellite valley. This creates

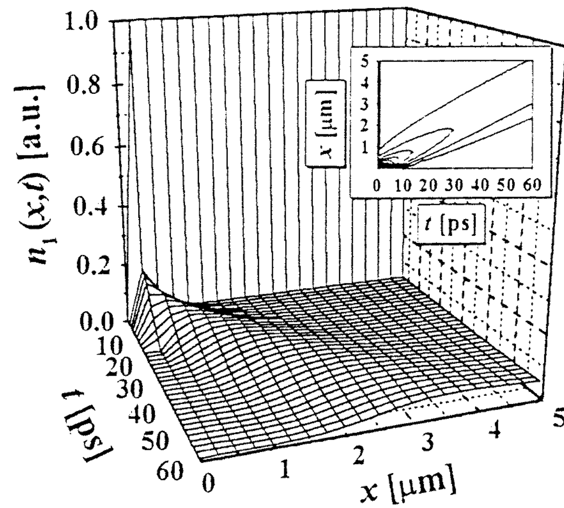

Figure 9. Spatial-temporal distribution of normalized concentration $n_1(x, t)$ in the central (Γ) valley for electric field $E = 30$ kV cm^{-1}.

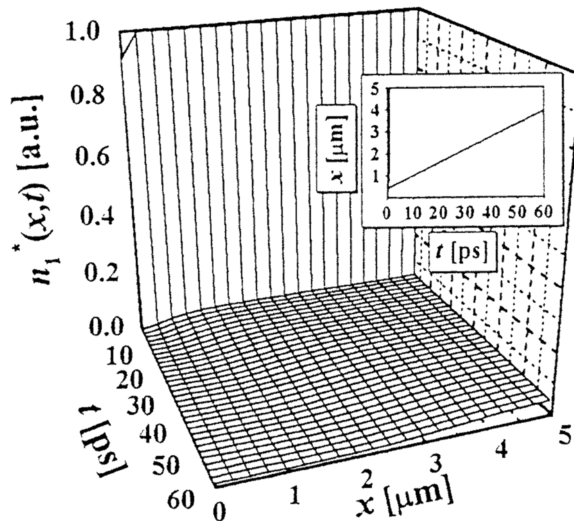

Figure 10. Spatial-temporal distribution of normalized concentration $n_1^*(x, t)$ in the central (Γ) valley for electric field $E = 30$ kV cm^{-1}.

an impression that the electron flow proceeds through the satellite valley with a velocity whose intensity is between the values ν_1 and ν_2.

Figures 3 and 4 show three-dimensional spatial-temporal profiles of the electrons concentration in the central valley for the electric field intensity of 5 kV cm^{-1}, obtained analytically and numerically, respectively. At a first glance it could appear that the solutions are identical. However, we can see the additional information in the added two-dimensional contour plots. In figure 3 we can easily see the boundaries of the regions I and IV, i.e. the straight lines $x = \nu_1 t$ and $x = \nu_2 t$, while in the numerical solution we can see only the boundary of the region I. Also, it can be seen that for $x > \nu_1 t$ the analytical and numerical

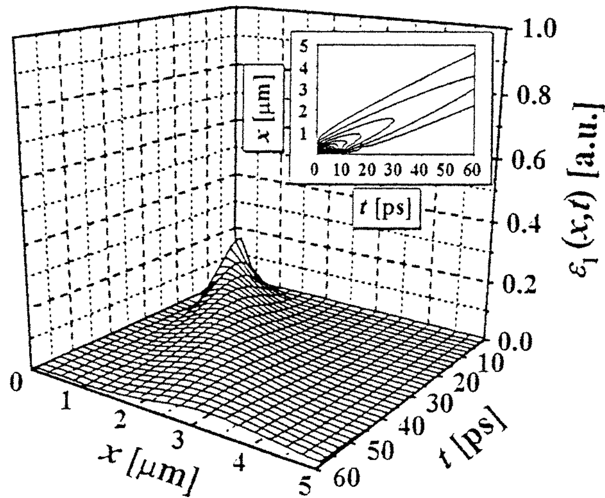

Figure 11. Spatial-temporal distribution of the difference $\epsilon_1(x, t)$ of the obtained concentrations in the central (Γ) valley for electric field $E = 30$ kV cm^{-1}.

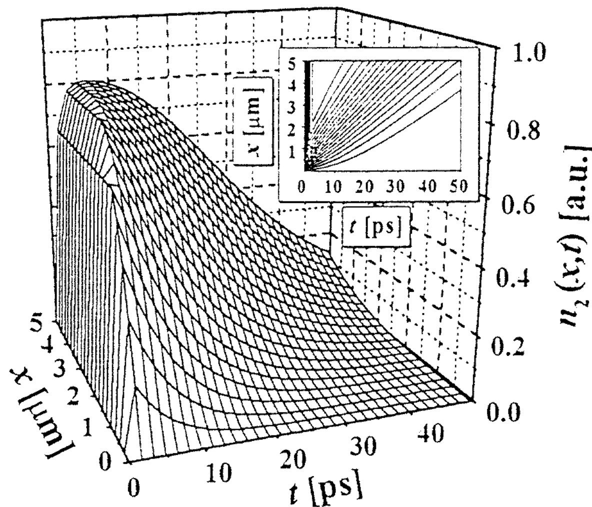

Figure 12. Spatial-temporal distribution of normalized concentration $n_2(x, t)$ in the satellite (X, L) valleys for electric field $E = 10$ kV cm^{-1}.

solution coincide for the most part, which is confirmed by figure 5 representing the spatial-temporal dependence of the difference $\epsilon_1(x, t)$ between the results obtained analytically and numerically. This difference shows clearly that the largest deviation appears near the straight boundary line $x = \nu_1 t$ in the regions II and III. It is obvious that the error is largest at the very beginning of the numerical procedure, where the 'stepped' boundary condition is posed. From the point of view of the transport processes, this means that the flow of the electrons which did not leave the central valley $(x > \nu_1, t)$ can be successfully described, while the discrepancy occurs for the transport of the electrons returning from the satellite valleys into the central one. The use of a more complex algorithm, for example the 'shock-capturing algorithm' (see [15, 16]) can minimize such errors for the cost of increased

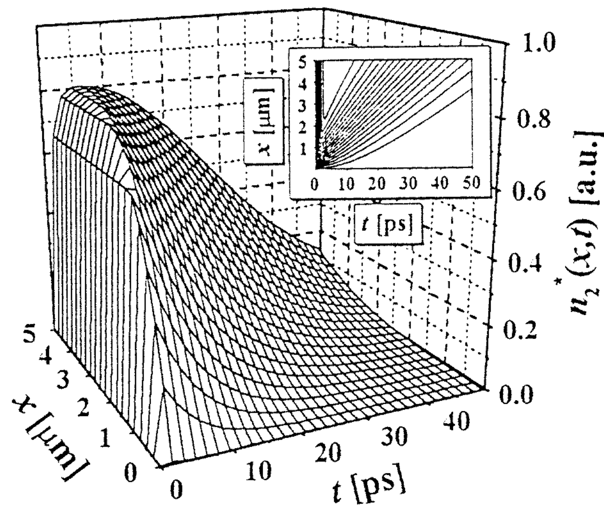

Figure 13. Spatial-temporal distribution of normalized concentration $n_2^*(x, t)$ in the satellite (X, L) valleys for electric field $E = 10$ kV cm^{-1}.

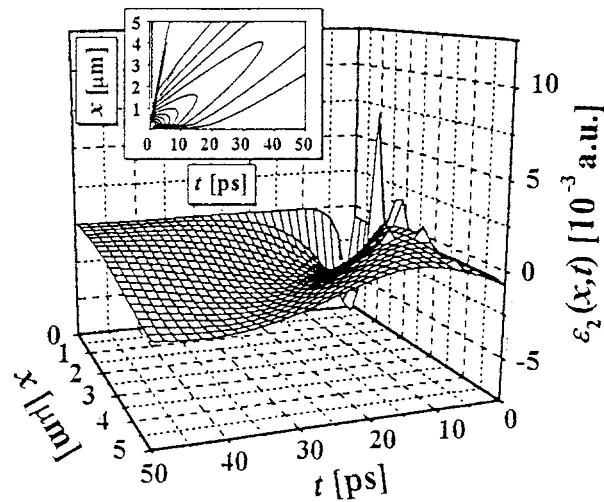

Figure 14. Spatial-temporal distribution of the difference $\epsilon_2(x, t)$ of the obtained concentrations in the satellite (X, L) valleys for electric field $E = 10$ kV cm^{-1}.

requirements for processor time and memory storage.

With an increase of the intensity of the electric field E the difference in behaviour between the analytical solution (figures 6 and 9) and numerical one (figures 7 and 10) for the concentration n_1 becomes more pronounced, although the absolute value of the difference ϵ_1 decreases (figures 8 and 11). The decrement of the absolute error is understandable, since due to the intensive intervalley transfer the values of the functions $n_1(x, t)$ and $n_1^*(x, t)$ sharply decrease (toward zero) after the initial moment which causes the decrease of their difference. However, the observed differences show that, when following the strong field activity transport, the applied difference scheme follows with increasing difficulties (or does

not follow at all) the changes in the regions II and III caused by electrons returning from the satellite valley into the central one.

The return of electrons from the satellite into the central valley can be seen in three-dimensional figures of the concentration n_1 as a 'hump' spreading through regions II and III. It can be explicitly seen for extremely strong ($E = 30$ kV cm^{-1}) electric fields (figure 9), while for a field of 10 kV cm^{-1} the obtained figure is the result of superposition of the spatial-temporal distributions of the carriers which remain for all the time transported through the central valley (region I) and the carriers returned from the satellite valleys into the central one (regions II and III).

By applying the exact solution we perceive the dynamics of the carrier transport and learn that the transport processes within the central valley proceed through two mechanisms. The primary mechanism is the flow of the carriers which do not leave the central valley during transport, while the other mechanism is based on the transport of carriers returned from the satellite valleys into the central valley. The second mechanism, however, cannot be perceived according to the simple numerical solution which 'smoothens' the consequences of this mechanism in the diagram showing the spatial-temporal dependence of electrons within the central valley.

Figures 12 and 13 show the solution for the carrier concentration in the satellite valley obtained analytically and numerically, respectively. Figure 14 shows that the absolute discrepancy of these solutions is extremely small. Of course, the discrepancy is largest at the beginning of the numerical procedure, the same as in the case of the central valley.

The satellite valley works like a 'reservoir' of electrons during transport. At the initial moment it accepts the electrons from the central valley, and then, after the number of electrons in the central valley is decreased due to transport, it returns the electrons into the central valley. In this case the numerical procedure is able to correctly follow the electron transport.

As stated in the introduction, the developed analytical procedure can be applied to those two- and three-dimensional models of semiconductor structures where the transport along one of the coordinates may be taken as dominant in comparison with the other ones. Such situations occur relatively frequently, as for example, in [3], where one-dimensional electron transport in a MESFET channel is analysed, as well as in the papers [15, 16], where the one-dimensional hydrodynamic model is applied to consider electron transport in an $n^+ - n - n^+$ structure. In a HEMT, electrons in the channel show large mobility only in the confinement plane, i.e. within the quantum well. The transport of these electrons proceeds only in the direction of the component of the electric field between the source and the drain along the confinement plane. Such transport can be considered as one-dimensional and thus it is possible to describe it by the presented model of transport equations, since quantum effects most significantly influence the electron confinement within the channel.

This analytical technique, unfortunately, does not permit an exact treatment of multidimensional models of semiconductor structures, regardless of the other conditions, since the system of equation (2) would contain at least one more spatial variable (y and/or z) and its partial derivative. Nevertheless, for such a system it is not possible to determine reliably in advance the existence of a solution which could be represented in an analytically closed form, as shown in [17].

Consequently, the previous analysis only describes the system of equation (2). Since the transport is one-dimensional, the boundary conditions can only be considered at the contacts of the device where an electric field is established. The equations from the system (2) are practically symmetrical with regard to the partial derivatives over the variables x and t.

Therefore, it is justified to expect that an analytical solution could also be found in the situation in which, relation (5) at the boundary $x = 0$, Dirichlet and Neumann's boundary conditions are simultaneously given, since the solution procedure would then be reduced to the already presented treatment of the Cauchy problem.

The presented analytical solution could be used for qualitative quantitative description of some other phenomena besides those mentioned, depending on their character, i.e. the possibility to model them, even only approximately, by equation (2), or for the different particular initial conditions of general type (5).

5. Conclusion

This work presents a detailed analysis of a general initial condition problem able to describe transport processes appearing in some two-valley semiconductor electron devices. A procedure is developed for one-dimensional exact explicit calculation of the function values (i.e. concentrations) n_1 and n_2 for arbitrary values of independent variables x and t, according to the expressions (26*a*–*d*), (30) and (33*a*–*d*). It is shown that a PDE system can be solved analytically (in quadratures) i.e. it can be reduced to the problem of calculating numerical values of integrals F_i and H_i, $(i = 1, 2)$, according to (27) and (34). Some of these integrals may be improper, but bearing in mind their convergence, some difficulties arising due to the singularity in the upper boundary can easily be overcome. However, in the proposed special case, describing the operation of p-i-n photodiodes, that problem disappears, and the obtained expressions become more compact and significantly simpler for numerical calculation. The achieved results are compared with the numerical solution obtained using the finite difference method by applying the so-called upwind scheme which is used most often for these kind of problems. The detailed analysis of the obtained error, with graphical illustrations for various representative values of parameters, is given. Beside the described advantages, the analytical treatment offers an additional possibility to independently calculate the concentrations n_1 and n_2 in an arbitrary position x and at an arbitrary moment t, while in the numerical solution there is an unavoidable limitation due to the discretization of the starting problem. The numerical method also requires all the previous calculations in the discretization mesh, which significantly increases the amount of time spent on calculations when compared with the implemented analytically obtained formulae.

The accuracy of calculating n_1 and n_2 is substantially improved in comparison with the methods of its calculation applied until now. The proposed insight into the transport mechanisms and the described phenomena becomes general, as opposed to the analyses known to the authors. The presented method also provides a new and very important possibility of optimization of the electric field parameter values, in order to obtain the desired optimal concentrations n_1 and n_2. Finally, the presented approach could be used in the analysis of electron transport and in certain real semiconductor devices where the electric field can be considered as homogeneous and stationary and for which the initial conditions of the presented general type (5) are valid. For example, in some situations it could also be possible to solve the equations of the hydrodynamic model if the corresponding coefficients were constant with respect to the independent variables, since the PDEs are of the same type as in the considered phenomenological model.

Finally, note that, bearing in mind the accuracy of the analytical and numerical procedure, the obtained solution could serve as a kind of 'standard' for assessing the efficiency of particular approximate methods for solution of PDE systems of the considered type.

Acknowledgment

The research of BDI was partly supported by The Mathematical Institute of SASA, Belgrade, project no 04M03.

References

[1] Yoshii A and Tomizawa M 1986 New approaches to submicron device modeling *Process and Device Modeling* ed W L Engl (Amsterdam: North-Holland) pp 195–227
[2] Blotekjaer K 1970 Transport equations for electrons in two-valley semiconductors *IEEE Trans. Electron Devices* **17** 38–47
[3] Stenzel R, Elschner H and Spallek R 1987 Numerical simulation of GaAs MESFETS including velocity overshoot *Solid-State Electron.* **30** 873–7
[4] Radunović J B and Gvozdić D M 1993 Nonstationary and nonlinear response of a p-i-n photodiode made of two-valley semiconductor *IEEE Trans. Electron Devices* **40** 1238–45
[5] Gvozdić D M 1997 Analysis of transfer function of metal–semiconductor–metal photodetector equivalent circuit *Appl. Phys. Lett.* **70** 286–8
[6] Courant R and Hilbert D 1968 *Methoden der mathematischen Physik II* 2nd edn (Berlin: Springer)
[7] Hellwig G 1977 *Partial Differential Equations* 2nd edn (Stuttgart: Teubner)
[8] Webster A G 1955 *Partial Differential Equations of Mathematical Physics* 2nd edn (New York: Dover)
[9] Farlow S J 1993 *Partial Differential Equations for Scientists and Engineers* 2nd edn (New York: Dover)
[10] Prudnikov A P, Brychkov Yu A and Marichev O I 1986 *Integrals and Series, Vol. 2: Special Functions* (New York: Gordon and Breach)
[11] Romberg W 1955 Vereinfachte numerische Integration *Det Kong. Norske Viden. Selskabs Forhand.* **28** 30–6
[12] Press W H, Flannery B P, Teukolsky S A and Vetterling W 1986 *Numerical Recipes* (Cambridge: Cambridge University Press)
[13] Walter W 1961 Fehlerabschätzungen bei hyperbolischen Differentialgleichungen *Arch. Rat. Mech. Anal.* **7** 249–72
[14] Strang G 1986 *Introduction to Applied Mathematics* (Wellesley: Wellesley-Cambridge Press)
[15] Fatemi E, Jerome J and Osher S 1991 Solution of the hydrodynamic device model using high-order nonoscillatory shock capturing algorithms *IEEE Trans. Comput.-Aided Des.* **10** 232–43
[16] Radunović D and Radunović J B 1994 Numerical simulation of two-valley semiconductor device model based on ENO shock capturing algorithm *Int. J. Numer. Modelling, Electron. Netw. Devices Fields* **7** 239–52
[17] Iričanin B and Gvozdić D 1997 On the analytic solution for the distribution of electron concentration in a two-valley semiconductor *Proc. 15th IMACS World Congress on Scientific Computation, Modelling and Applied Mathematics* vol 3, ed A Sydow (Berlin: Wissenschaft & Technik) pp 581–6